Available online at www.sciencedirect.com
SCIENCE DIRECT®
Inorganica Chimica Acta 341 (2002) 91–98
Inorganica Chimica Acta
www.elsevier.com/locate/ica

# Coordinatively and electronically unsaturated tris(trimethylsilyl)silyl complexes of manganese and iron

Richard H. Heyn, T. Don Tilley *

*Department of Chemistry, University of California, Berkeley, CA 94720-1460, USA*

Received 2 May 2002; accepted 8 July 2002

This paper is dedicated to Ken Raymond, a great friend and colleague, on the occasion of his 60th birthday.

**Abstract**

The neutral, bis(silyl) complexes $M[Si(SiMe_3)_3]_2(THF)_n$ (**3**, M = Mn, $n = 2$; **4**, M = Fe, $n = 1$) represent reactive, useful starting materials for the synthesis of various silyl derivatives of Mn and Fe. The reaction of **3** with dmpe (dmpe = $Me_2PCH_2CH_2PMe_2$) produced the yellow–orange complex $Mn[Si(SiMe_3)_3]_2$(dmpe), which was characterized by X-ray crystallography as possessing Mn–Si distances of 2.643(4) and 2.642(3) Å. A related benzophenone complex, $Mn[Si(SiMe_3)_3]_2(OCPh_2)_2$, is dark blue in color but possesses neutral ketone ligands (by IR spectroscopy and X-ray crystallography). The reaction of $[NEt_4]\{Fe[Si(SiMe_3)_3]_2Cl\}$ with CO gave $[NEt_4]\{Fe(CO)_3[Si(SiMe_3)_3]_2Cl\}$, and the reaction of **3** with CNXyl (Xyl = 2,6-$Me_2$–$C_6H_3$) produced $Mn[Si(SiMe_3)_3]_2$(CNXyl)(THF) and the reduced manganese complex $(XylNC)_5MnSi(SiMe_3)_3$.


*Keywords:* Silyl complexes; Manganese complexes; Iron complexes; Coordinatively unsaturated

## 1. Introduction

In recent years, transition-metal silicon chemistry has received increased attention as new stoichiometric and catalytic processes based on metal–silicon bonded species have been developed [1]. The discovery of new reactivity patterns for transition-metal silyl complexes will rely to some degree on development of new classes of compounds characterized by high reactivity. To date, most transition-metal silyl derivatives are based on 'traditional' coordination spheres featuring coordinative unsaturation supported by cyclopentadienyl, phosphine, or π-acid ligands. With the expectation that coordinative unsaturation and hitherto unexplored coordination geometries might lead to new types of reactions for metal–silicon bonded compounds, we have explored routes to electron-deficient silyl complexes with exceedingly low coordination numbers. In a previous report, we described the synthesis of high-spin three- and four-coordinate silyl complexes of Cr, Mn and Fe. These complexes were prepared by reactions of $(THF)_3LiSi(SiMe_3)_3$ with metal dihalides, which allowed isolation of complexes of the types $\{M[Si(SiMe_3)_3]_2Cl\}^-$ (M = Cr, Mn, Fe; DME = 1,2-dimethoxyethane), $[(Me_3Si)_3Si]_2M(DME)$ (M = Mn, Fe) and $[(Me_3Si)_3Si]_2Fe(OEt_2)$ [2]. To characterize the chemical behavior of these complexes, we have studied their reactions with small molecules that coordinate to the metal and expand the coordination spheres. Here we describe new reactions of manganese and iron bis(silyl) complexes, and the molecular structures of two four-coordinate Mn silyl complexes.

## 2. Experimental

All manipulations were performed under an inert atmosphere of $N_2$ or Ar, using either a high-vacuum swivel-frit apparatus, standard Schlenk techniques, or a Vacuum Atmospheres glove-box. Dry, oxygen-free solvents were employed throughout. Elemental analyses were performed by Mikroanalytiches Labor Pascher

* Corresponding author. Fax: +1-510-642 8940
*E-mail address:* tdtilley@socrates.berkeley.edu (T.D. Tilley).

0020-1693/02/$ - see front matter 
PII: S0020-1693(02)01182-9

(Germany) or Schwarzkopf Microanalytical Laboratories. Infrared spectra were recorded on a Perkin–Elmer 1330 spectrometer. Electronic spectra were recorded on an IBM 9420 UV–Vis spectrophotometer. NMR spectra were obtained with a GE-QE 300 instrument at 300 or 75.5 MHz ($^1$H or $^{13}$C, respectively) or on a Varian EM 390 (90 MHz, $^1$H). Benzophenone was recrystallized from ethanol and dried under vacuum before use. $Li(THF)_3Si(SiMe_3)_3$ was prepared according to a published procedure [3].

### 2.1. $Li(THF)_3\{Mn[Si(SiMe_3)_3]_2Cl\}$ (1)

Both $MnCl_2$ (1.30 g, 10.3 mmol) and $Li(THF)_3Si(SiMe_3)_3$ (10.1 g, 20.6 mmol) were combined in a 100 ml flask. The solids were cooled to −78 °C and $Et_2O$ (50 ml) was condensed onto the solids. The mixture was warmed to room temperature (r.t.) and the heterogeneous dark yellow mixture was stirred for 2.5 h. The mixture was filtered, and the insoluble material was washed with $Et_2O$ (2 × 15 ml). The combined ether solutions were concentrated to 15 ml and then cooled to −78 °C. Addition of pentane (35 ml) precipitated a yellow solid, which was isolated by filtration at −78 °C to give 7.52 g (9.37 mmol, 91%) of product. The amount of THF present can vary with the length of drying time after isolation of the product. The compound was shown to contain lithium by a flame test. As reported previously, compounds of this type sometimes exhibit consistently low and variable carbon analyses (possibly due to the formation of stable carbides during the combustion analysis) [2], and this was observed for compound **1**. Thus, the composition of the complex was confirmed by an analysis of its hydrolytic degradation products. To a benzene-$d_6$ solution of the product and a weighed amount of ferrocene standard was added an excess of water. A $^1$H NMR spectrum of the resulting solution revealed complete hydrolysis, and integration of the resonances for $HSi(SiMe_3)_3$ and THF against that of the standard established the stoichiometry of **1**.

### 2.2. $Mn[Si(SiMe_3)_3]_2(THF)_2$ (3)

A 100 ml flask was charged with $Li(THF)_3\{MnCl[Si(SiMe_3)_3]_2\}$ (8.05 g, 10.3 mmol) and $Me_3SiOSO_2CF_3$ (3.0 ml, 15.5 mmol). The mixture was cooled to −78 °C and $Et_2O$ (75 ml) was condensed into the flask. The reaction mixture was allowed to warm to r.t., and the resulting yellow solution was stirred for 3 h. The volatile material was removed, and pentane (75 ml) was added. The insoluble material was removed by filtration and washed with pentane (3 × 20 ml). After concentration to 30 ml, the yellow solution was cooled to −78 °C, and filtration afforded 3.28 g (4.84 mmol) of pale yellow microcrystals. Repeating the isolation procedure gave 2.80 g (4.35 mmol) of crystals in a second crop, for a total yield of 90%. The amount of THF in the product varies somewhat with drying time. Recrystallization from pentane with a small amount of added THF allowed isolation of microcrystals of analytically pure **3**. *Anal.* Calc. for $C_{26}H_{70}MnO_2Si_8$: C, 45.0; H, 10.2. Found: C, 44.2; H, 10.1%. Melting point (m.p.) (dec.): 140–142 °C. Evans' moment: 5.7 BM. IR (CsI, Nujol, $cm^{-1}$): 1292w, 1252w sh, 1237m, 1072w, 1029m, 857m sh, 834br s, 742w, 731w, 676m, 621m.

### 2.3. $Fe[Si(SiMe_3)_3]_2(THF)$ (4)

The procedure was analogous to that for **3**, starting with $Li(THF)_3\{FeCl[Si(SiMe_3)_3]_2\}$ (0.91 g, 1.20 mmol), $Me_3SiOSO_2CF_3$ (0.5 ml, 2.6 mmol), and $Et_2O$ (35 ml). The blue–purple solution was stirred at r.t. for 2 h. Two crops of dark green crystals totaling 0.47 g (0.75 mmol, 62%) were obtained from cooled pentane solutions. Analysis of the hydrolytic degradation products, as described for **1**, established the stoichiometry of **4**. IR (CsI, Nujol, $cm^{-1}$): 1255w sh, 1240m, 1037w sh, 1018m, 832br s, 743w, 732w, 680m, 621m, 431w, 394w.

### 2.4. $Mn[Si(SiMe_3)_3]_2(dmpe)$ (5)

A 25 ml flask was charged with $Mn[Si(SiMe_3)_3]_2(THF)_2$ (0.39 g, 0.56 mmol) and cooled to −78 °C. Pentane (20 ml) was condensed into the flask, followed by the addition of dmpe (0.1 ml, 0.60 mmol) via syringe. Immediately the reaction became bright yellow. The mixture was warmed to r.t. and after 3 h, the volatile material was removed under vacuum. The yellow residue was extracted with $Et_2O$ (15 ml) to remove a small amount of black solid. After removal of the $Et_2O$, crystallization from pentane provided two crops of yellow–orange crystals totalling 0.33 g (0.47 mmol, 84%). *Anal.* Calc. for $C_{24}H_{70}MnP_2Si_8$: C, 41.2; H, 10.1. Found: C, 40.9; H, 10.1%. M.p. (dec.): 196–199 °C. Evans' Moment: 6.1 BM. IR (CsI, Nujol, $cm^{-1}$): 1409w, 1302w, 1288w, 1250w, 1236s, 947w, 934w, 830vs, 737w, 704w, 671m, 620m, 419w, 385w.

### 2.5. $Mn[Si(SiMe_3)_3]_2(OCPh_2)_2$ (6)

A 50 ml flask was charged with $Mn[Si(SiMe_3)_3]_2(THF)_2$ (1.44 g, 2.1 mmol) and $Ph_2CO$ (0.75 g, 4.1 mmol). The solids were cooled to −78 °C, and pentane (40 ml) was condensed into the flask. The purple mixture was warmed to r.t. and stirred for 1.25 h. After the volatiles were removed in vacuo, the purple residue was extracted with pentane (3 × 40 ml). Cooling and concentrating the resulting purple solution resulted in isolation of three crops of product in a combined yield of 1.75 g (1.9 mmol, 92%). *Anal.* Calc. for $C_{44}H_{74}MnO_2Si_8$: C, 57.8; H, 8.15. Found: C, 57.7; H, 8.19%. M.p.: 118–122 °C. Evans' Moment: 5.7 BM.

UV–Vis (pentane, nm): 640 (1000), 619 (1300), 451 (800), 376 (1100), 313 (2700), 248 (60 000), 220 (28 000). IR (CsI, Nujol, $cm^{-1}$): 1623m, 1611m, 1594m, 1571m, 1450m, 1317m, 1327m, 1317m, 1290m, 1251m sh, 1237m, 1180w, 1159w, 1076w, 1030w, 1001w, 946w, 926w, 831s, 762m, 731w, 701s, 678m, 638m, 621m, 424w.

### 2.6. [NEt4]{Fe(CO)3[Si(SiMe3)3]2Cl} (7)

A 60 ml Schlenk flask was charged with $[NEt_4]\{FeCl[Si(SiMe_3)_3]_2\}$ (1.25 g, 1.74 mmol) and $Et_2O$ (40 ml). The resulting purple mixture was then transferred to a Fischer–Porter bottle and pressurized to 60 psi of CO. After stirring for 4 h, the excess CO was removed, and the orange–red mixture was transferred to a Schlenk flask. The volatiles were removed, and the resulting orange–red residue was extracted with $CH_3CN$ (40 ml). After filtration, the solution was cooled to −35 °C, which subsequently provided two crops of orange–red crystals, totaling 1.09 g (1.36 mmol, 78%). *Anal.* Calc. for $C_{29}H_{74}ClFeNO_3Si_8$: C, 43.5; H, 9.31; Cl, 4.43; N, 1.75. Found: C, 43.1; H, 9.31; Cl, 4.08; N, 1.81%. M.p. (dec.): 147–149 °C. $^1$H NMR (acetonitrile-$d_3$, 90 MHz, 30 °C): $\delta$ 0.26 (s, 54H, SiC$H_3$), 1.21 (m, 12H, NCC$H_3$), 3.18 (q, $^3J_{HH} = 7$ Hz, 8H, NC$H_2$). $^{13}C\{^1H\}$ NMR (acetonitrile-$d_3$, 75.5 MHz, 24 °C): $\delta$ 4.90 (Si$CH_3$), 8.43 (NC$CH_3$), 53.6 (N$CH_2$), 216.9 ($CO$), 227.5 ($CO$). IR (CsI, Nujol, $cm^{-1}$): 1953s, 1921s, 1833m, 1259m, 1239m, 1169w, 860m sh, 839br s, 800m, 677m, 640w, 620m, 599m, 592m sh.

### 2.7. Reaction of Mn[Si(SiMe3)3]2(THF)2 with CN(2,6-Me2C6H3); synthesis of Mn[Si(SiMe3)3]2[CN(2,6-Me2C6H3)](THF) (8) and Mn[Si(SiMe3)3][CN(2,6-Me2C6H3)]5 (9)

A 50 ml flask was charged with $Mn[Si(SiMe_3)_3]_2(THF)_{1.6}$ (0.45 g, 0.67 mmol). The solid was cooled to −78 °C, and pentane (20 ml) was condensed into the flask. In a separate flask, $CN(2,6\text{-}Me_2C_6H_3)$ (CNXyl; 0.26 g, 2.00 mmol) was dissolved in pentane (20 ml), and the clear solution was transferred via cannula to the cooled suspension. The reaction mixture immediately became red and was stirred at −78 °C for 1 h. The reaction was then warmed to r.t. and the now homogeneous dark red solution was stirred for 1.5 h. After 0.5 h, an orange precipitate began to form. The reaction mixture was concentrated to 5 ml, and the precipitate was removed by filtration and then washed with pentane (2 × 5 ml), which provided 0.17 g of yellow solid. Cooling the filtrate to −78 °C subsequently provided 0.17 g of red powder. Neither product gave consistent results by combustion analysis. Use of greater amounts of CNXyl in the synthesis increased the yield of the yellow product, but the yield of this species was not optimized. For the red product (**8**), hydrolytic degradation with a standard provided a stoichiometry consistent with $Mn[Si(SiMe_3)_3]_2(CNXyl)(THF)$. IR (CsI, Nujol, $cm^{-1}$): 2160m, 2018w, 1981w, 1295w, 1249m sh, 1235m, 1167w, 1030w, 970w, 855s sh, 832vs, 775m, 742m, 731w, 678m, 621m, 434w, 395w. The air-stable yellow product (**9**) was characterized by NMR spectroscopy and mass spectrometry. Mass spectroscopy: Calc. for $C_{54}H_{72}MnN_5Si_4$: 957.4254. Found: 957.4221%. M.p. (dec.): 221–231 °C. $^1$H NMR (benzene-$d_6$, 300 MHz, 24 °C): $\delta$ 0.66 (s, 27H, SiC$H_3$), 2.09 (s, 6H, $o$-C$H_3$), 2.51 (s, 24H, $o$-C$H_3$), 6.61 (m, 3H, $C_6H_3$), 6.75 (s, 12H, $C_6H_3$). IR (CsI, Nujol, $cm^{-1}$): 2118s, 1998br vs, 1589m, 1231m, 1188w, 1162w, 1092w, 1030w, 919w, 859m, 831s, 769s, 675m sh, 663s, 621w, 600m, 592m, 552w, 505m, 492m sh, 399w.

### 2.8. Structure determination of 5

Crystallographic data are summarized in Table 1. A yellow–orange crystal was mounted under $N_2$ in a random orientation in a glass capillary and flame-sealed. Centering of 24 randomly selected reflections with $15 \leq 2\theta \leq 30°$ provided unit cell data. The selection of the monoclinic cell was confirmed by axial photographs. The data were corrected for Lorentz and polarization effects, and for a decay in the intensity of three check reflections of 2.5%. A semi-empirical absorption correction based on the Ψ-scan method was employed. Systematic absences uniquely determined the space group as $P2_1/c$. The structure was solved via a Patterson map and refined by full-matrix least-squares methods. Due to a lack of data, only the Mn, P, and Si atoms were

Table 1
Crystallographic data for $Mn[Si(SiMe_3)_3]_2(OCPh_2)_2$ (**5**)

| | |
|---|---|
| Chemical formula | $C_{24}H_{70}Si_8P_2Mn$ |
| Formula weight | 700.4 |
| $T$ (°C) | 20 |
| Space group | $P2_1/c$ |
| $a$ (Å) | 13.125 (3) |
| $b$ (Å) | 18.191 (5) |
| $c$ (Å) | 19.486 (5) |
| $\beta$ (°) | 104.80(2) |
| $V$ (Å$^3$) | 4498 (2) |
| $Z$ | 4 |
| $\rho_{calc}$ (g $cm^{-1}$) | 1.034 |
| $\mu$ ($mm^{-1}$) | 0.574 |
| $\lambda$ (Mo Kα) (Å) | 0.71073 |
| Data/parameters | 12.2 |
| Weighting scheme | $w^{-1} = \sigma^2(F) + 0.0006F^2$ |
| Scan type | Wycoff |
| Scan speed (° $min^{-1}$ in $\omega$) | 5.00–29.00 |
| $R_F$ (%) [a] | 6.34 |
| $R_{wF}$ (%) [b] | 7.01 |
| Goodness-of-fit | 1.56 |

[a] $R_F = \Sigma||F_o| - |F_c||/\Sigma|F_o|$.
[b] $R_{wF} = [\Sigma\ w(|F_o| - |F_c|)^2/\Sigma\ w|F_o|^2]^{1/2}$.

refined anisotropically. The hydrogen atoms were placed in idealized, calculated positions ($d$(C–H) = 0.96 Å), with a fixed thermal parameter approximately equal to 1.2 times the isotropic thermal of the attached carbon atom.

### 2.9. Structure determination of **6**

Crystallographic data are summarized in Table 2. A deep purple crystal was mounted under $N_2$ in a random orientation in a glass capillary and flame-sealed. Centering of 25 randomly selected reflections with $15 \leq 2\theta \leq 30^\circ$ provided unit cell data. The selection of the tetragonal cell was confirmed by axial photographs. The data were corrected for Lorentz and polarization effects, and for a decay in the intensity of three check reflections of 1.5%. A profile fitting procedure was applied to the data to enhance the quality of weak reflections. A semi-empirical absorption correction based on the Ψ-scan method was employed. Systematic absences uniquely determined the space group as $I4_1cd$ The structure was solved via direct methods and refined by full-matrix least-squares methods. One reflection with large $\Delta/\sigma$ was removed from the final refinement. Due to a lack of data, only the Mn, Si(1), and Si(5) atoms were refined anisotropically. The hydrogen atoms were placed in idealized, calculated positions ($d$(C–H) = 0.96 Å), with a fixed thermal parameter approximately equal to 1.2 times the isotropic thermal of the attached carbon atom. All calculations employed the Siemens SHELXTL-PLUS computing package (Siemens Analytical X-ray Instruments, Inc., Madison, WI).

Table 2
Crystallographic data for $Mn[Si(SiMe_3)_3]_2(dmpe)$ (**6**)

| | |
|---|---|
| Chemical formula | $C_{44}H_{74}MnO_2Si_8$ |
| Formula weight | 914.7 |
| $T$ (°C) | 22 |
| Space group | $I4_1cd$ |
| $a$ (Å) | 28.562 (4) |
| $c$ (Å) | 27.792 (7) |
| $V$ (Å$^3$) | 22672 (9) |
| $Z$ | 16 |
| $\rho_{calc}$ (g cm$^{-1}$) | 1.072 |
| $\mu$ (mm$^{-1}$) | 0.418 |
| $\lambda$ (Mo Kα) (Å) | 0.71073 |
| Data/parameters | 8.3 |
| Weighting scheme | $w^{-1} = \sigma^2(F) + 0.0024F^2$ |
| Scan type | Wycoff |
| Scan speed (° min$^{-1}$ in $\omega$) | 2.00–14.65 |
| $R_F$ (%) [a] | 6.67 |
| $R_{wF}$ (%) [b] | 8.79 |
| Goodness-of-fit | 1.37 |

[a] $R_F = \Sigma||F_o| - |F_c||/\Sigma|F_o|$.
[b] $R_{wF} = [\Sigma\ w(|F_o| - |F_c|)^2/\Sigma\ w|F_o|^2]^{1/2}$.

## 3. Results and discussion

In general, reactions of $(THF)_3LiSi(SiMe_3)_3$ with $MnCl_2$ or $FeCl_2$ in an ethereal solvent produce anionic complexes of the type $[Li(ether)_x]\{M[Si(SiMe_3)_3]_2Cl\}$. We previously described the DME derivatives $[Li(DME)_2]\{M[Si(SiMe_3)_3]_2Cl\}$ (M = Mn, Fe) [2], and analogous reactions in THF give the corresponding adducts $[Li(THF)_3]\{M[Si(SiMe_3)_3]_2Cl\}$ (**1**, M = Mn; **2**, M = Fe). These anionic species may be converted to the neutral complexes $M[Si(SiMe_3)_3]_2(DME)$ (M = Mn, Fe) and $Fe[Si(SiMe_3)_3]_2(OEt_2)$ [2], but we have found the THF adducts **3** and **4** to be more synthetically useful. These compounds were prepared by reactions of **1** and **2** with $Me_3SiOTf$ ($OTf^-$ = triflate), as shown in Eq. (1). Complexes **3** and **4**, which were isolated in 90 and 62% yields, respectively, are paramagnetic and, therefore, little information can be obtained by NMR spectroscopy. Furthermore, our experience has shown that combustion analyses of these compounds often provide low and variable values for carbon, presumably due to the formation of carbides which do not burn completely during the analysis. Therefore, in some cases, an alternative and reliable method of analysis was employed involving destructive hydrolysis of the complexes to liberate the coordinated base and the silyl ligand as $HSi(SiMe_3)_3$. Integration of the resonances for the hydrolysis products against an internal standard (usually ferrocene) provided the stoichiometry of the compound. Further characterization was based on infrared spectroscopy, which revealed absorptions due to the ligands present. Particularly diagnostic are three characteristic absorptions between 600 and 900 cm$^{-1}$ due to the -Si(SiMe$_3$)$_3$ groups. For example, for **3** these absorptions appear at 834, 676 and 621 cm$^{-1}$.

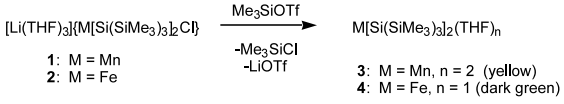

(1)

### 3.1. Reactions of $Mn[Si(SiMe_3)_3]_2(THF)_2$ (**3**) with phosphines

Addition of monodentate phosphines ($\leq$3 equiv. of $PMe_3$ or $P(OMe)_3$) to **3** produced materials that possess the stoichiometry $Mn[Si(SiMe_3)_3]_2(PR_3)_x(THF)_{1-x}$ (by NMR analysis of the hydrolysis products). It is difficult to rigorously characterize the products of these reactions as single compounds or as mixtures of **3** and $Mn[Si(SiMe_3)_3]_2(PR_3)_x$, and we were not able to obtain X-ray quality crystals. We, therefore, more closely examined the reaction of **3** with the bidentate phosphine $Me_2PCH_2CH_2PMe_2$ (dmpe), which provided good yields of the yellow–orange complex **5** (Eq. (2)). This

compound may also be prepared from the reaction of **1** with dmpe, albeit in lower yields.

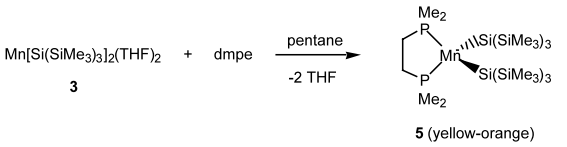


(2)

Complex **5** has a $\mu_{eff}$ value of 6.1 BM (determined by the Evans method [4]), which is nearly the same as the value observed for **3** (5.7 BM) and consistent with a high-spin configuration. Infrared absorptions attributed to the silyl ligands in **5** appeared at 830, 671 and 620 $cm^{-1}$.

### 3.2. Structure of $Mn[Si(SiMe_3)_3]_2(dmpe)$ (5)

An ORTEP diagram of the molecular structure of **5** is given in Fig. 1, and bond distances and angles appear in Table 3. The high-spin nature of **5** is reflected in the Mn–Si distances of 2.643(4) and 2.642(3) Å, which are considerably longer than the longest previously reported Mn–Si distance (2.564 (6) Å for the six-coordinate and low-spin $(CO)_5MnSi(SiMe_3)_3$ [5]). Other Mn–Si distances range from 2.31 to 2.50 Å [1a,1b]. Compound **5** has a distorted tetrahedral coordination geometry, with a Si–Mn–Si angle (133.8(1)°) which is undoubtedly due to the steric bulk of the silyl ligand. The Mn–P distances average to 2.66 Å, and are similar to Mn–P bond lengths found in other high-spin Mn(II) complexes. For example, the Mn–P distance in $MnBr_2(dmpe)_2$ is 2.655(4) Å [6] and in $Mn[TeSi(SiMe_3)_3]_2(dmpe)$ it is 2.600(3) Å [7]. For $Mn[CH(SiMe_3)_2]_2(dmpe)$ this distance is even longer at 2.775(4) Å [8]. The P–Mn–P angle in **5** of 78.1(1) is also comparable with the corresponding angles reported for the above two complexes. The P–Mn–Si angles show less distortion and are near the tetrahedral value (average 107.7(1)°).

As in $[NEt_4]\{Fe[Si(SiMe_3)_3]_2Cl\}$ [2], the $-Si(SiMe_3)_3$ ligands of **5** exhibit a distorted tetrahedral environment about the donor Si atoms. The Mn–Si(1)–Si angles are 110.5(2), 112.4(1) and 121.6(2) Å and the Mn–Si(5)–Si angles are 112.8(1), 114.3(2) and 117.5(2)°. Therefore,

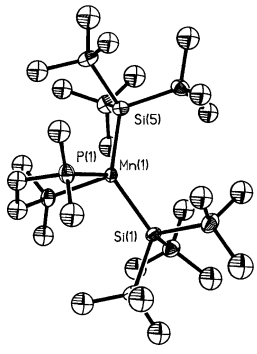


Fig. 1. ORTEP view of $Mn[Si(SiMe_3)_3]_2(dmpe)$ (**5**).

Table 3
Selected bond distances (Å) and angles (°) for **5**

| | | | |
|---|---|---|---|
| *Bond distances* | | | |
| Mn(1)–P(1) | 2.675(3) | Mn(1)–Si(1) | 2.643(4) |
| Mn(1)–P(2) | 2.647(4) | Mn(1)–Si(5) | 2.642(3) |
| Si(1)–Si(2) | 2.334(6) | Si(5)–Si(6) | 2.345(5) |
| Si(1)–Si(3) | 2.351(5) | Si(5)–Si(7) | 2.361(5) |
| Si(1)–Si(4) | 2.367(5) | Si(5)–Si(8) | 2.339(5) |
| *Bond angles* | | | |
| P(1)–Mn(1)–P(2) | 78.1(1) | P(1)–Mn(1)–Si(1) | 108.0(1) |
| P(2)–Mn(1)–Si(1) | 106.0(1) | P(1)–Mn(1)–Si(5) | 109.5(1) |
| P(2)–Mn(1)–Si(5) | 107.3(1) | Si(1)–Mn(1)–Si(5) | 133.8(1) |
| Mn(1)–Si(1)–Si(2) | 110.5(2) | Mn(1)–Si(1)–Si(3) | 112.4(1) |
| Si(2)–Si(1)–Si(3) | 104.6(2) | Mn(1)–Si(1)–Si(4) | 121.6(2) |
| Si(2)–Si(1)–Si(4) | 102.0(2) | Si(3)–Si(1)–Si(4) | 104.1(2) |
| Mn(1)–Si(5)–Si(6) | 117.5(2) | Mn(1)–Si(5)–Si(7) | 114.3(2) |
| Si(6)–Si(5)–Si(7) | 103.5(2) | Mn(1)–Si(5)–Si(8) | 112.8(1) |
| Si(6)–Si(5)–Si(8) | 101.4(2) | Si(67)–Si(5)–Si(8) | 106.0(2) |

these distortions are not as severe as those observed in $[NEt_4]\{Fe[Si(SiMe_3)_3]_2Cl\}$, despite the fact that bidentate dmpe is more sterically demanding than a chloride ligand. However, the Si–Si distances in **5** (2.33–2.35 Å) are about 0.02 Å longer than those found in $[NEt_4]\{Fe[Si(SiMe_3)_3]_2Cl\}$.

### 3.3. Reactions of $Mn[Si(SiMe_3)_3]_2(THF)_2$ (3) with ketones

A few reports have described the insertion of organic carbonyl compounds into M–Si bonds. Whereas low-valent manganese and iron silyl complexes are known to insert organic carbonyls to give α-siloxy alkyl derivatives [9], $(\eta^5\text{-}C_5Me_5)Cl_3TaSiMe_3$ adds to C=O double bonds via nucleophilic transfer of the silyl group to the carbonyl carbon atom [10]. Given the unique properties of **3** as a coordinatively unsaturated, high-spin silyl complex, we were interested in examining possible insertion reactions with ketones and aldehydes.

Reactions of **3** with 1 equiv. of acetone or acetophenone at various stoichiometries did not yield crystalline materials that could be identified as pure products. With 1:1 ratios of reactants, powders were isolated which exhibited the stoichiometry $Mn[Si(SiMe_3)_3]_2(THF)$(ketone) (ketone = $Me_2CO$, PhMeCO), as determined by destructive hydrolysis. In these hydrolysis reactions, the corresponding ketone was released. Interestingly, while complexes of acetone are yellow, complexes of acetophenone are considerably darker and were isolated as deep purple powders.

The reaction of **3** with 2 equiv. of benzophenone provided a pure compound that was characterized as the adduct $Mn[Si(SiMe_3)_3]_2(OCPh_2)_2$ (**6**), isolated in 92% yield as dark blue crystals from pentane (Eq. (3)). The magnetic moment (5.7 BM) indicates that the complex has an electronic structure similar to those of the other

$Mn[Si(SiMe_3)_3]_2$ derivatives. The infrared spectrum of **6** contains absorbances at 1623 and 1611 $cm^{-1}$ which are assigned to the C=O stretches of the coordinated benzophenone ligands. These values may be compared with the C=O stretching frequencies for free benzophenone (1659 $cm^{-1}$) and for the orthometallated complex $(CO)_4MnOCPh(C_6H_4)$ (1519 $cm^{-1}$) [11]. These data indicate that the C=O bonds in **6** possess a high degree of double bond character, as might be expected for a coordination complex of the electron-deficient Mn(II) center.

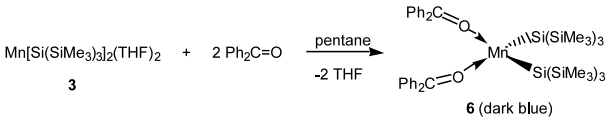


(3)

The deep blue color of **6** is very similar to that of the benzophenone ketyl radical. The UV–Vis spectrum of **6** contains bands at 640 nm ($\varepsilon = 1000\ M^{-1}\ cm^{-1}$) and 313 nm ($\varepsilon = 2700\ M^{-1}\ cm^{-1}$), which are close in energy to bands reported for the benzophenone radical anion in aqueous solution, at 615 nm ($\varepsilon = 6100\ M^{-1}\ cm^{-1}$) and 339 nm ($\varepsilon = 20\,000\ M^{-1}\ cm^{-1}$) [12]. Additionally, the carbon-centered radical $(^tBu_3SiO)_3TiOPh_2C^{\bullet}$ exhibits an absorption at 646 nm ($\varepsilon = 1800\ M^{-1}\ cm^{-1}$) [13], and the benzophenone ketyl complex $Ca(OCPh_2)_2(HMPA)_3$ exhibits an absorption at 635 nm [14]. Based on these comparisons, it seems possible that at least some of the unpaired electron density in high-spin **6** is delocalized into the π-system of the coordinated benzophenone.

### 3.4. Structure of $Mn[Si(SiMe_3)_3]_2(OCPh_2)$ (6)

An ORTEP view of the molecular structure of **6** is given in Fig. 2, and bond distances and angles are listed in Table 4. The complex exhibits a tetrahedral coordination geometry, which is distorted by the steric demands of the bulky silyl groups. Thus the Si–Mn–Si angle is 133.3(2)°, whereas the O–Mn–O angle is only 90.3(5)° and the O–Mn–Si angles average to 106°. The Mn–Si

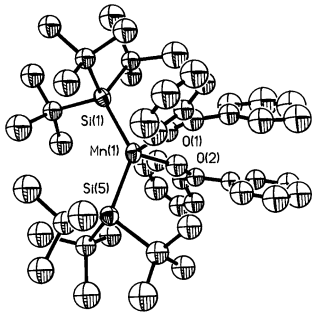


Fig. 2. ORTEP view of $Mn[Si(SiMe_3)_3]_2(OCPh_2)_2$ (**6**).

Table 4
Selected bond distances (Å) and angles (°) for **6**

| | | | |
|---|---|---|---|
| *Bond distances* | | | |
| Mn(1)–Si(1) | 2.642(6) | Mn(1)–Si(5) | 2.662(6) |
| Mn(1)–O(1) | 2.13(1) | Mn(1)–O(2) | 2.14(1) |
| Si(1)–Si(2) | 2.354(8) | Si(1)–Si(3) | 2.366(8) |
| Si(1)–Si(4) | 2.354(8) | Si(5)–Si(7) | 2.355(7) |
| Si(5)–Si(6) | 2.337(8) | Si(5)–Si(8) | 2.355(9) |
| O(1)–C(1) | 1.24(2) | O(2)–C(101) | 1.29(2) |
| C(1)–C(2) | 1.51(2) | C(101)–C(102) | 1.43(2) |
| C(1)–C(8) | 1.45(3) | C(101)–C(108) | 1.44(2) |
| *Bond angles* | | | |
| Si(1)–Mn(1)–Si(5) | 133.3(2) | Si(1)–Mn(1)–O(1) | 102.1(4) |
| Si(5)–Mn(1)–O(1) | 106.9(4) | Si(1)–Mn(1)–O(2) | 111.1(4) |
| Si(5)–Mn(1)–O(2) | 104.7(4) | O(2)–Mn(1)–O(2) | 90.3(5) |
| Mn(1)–Si(1)–Si(2) | 108.4(2) | Mn(1)–Si(1)–Si(3) | 122.1(2) |
| Mn(1)–Si(1)–Si(4) | 112.3(3) | Si(2)–Si(1)–Si(3) | 102.4(3) |
| Si(2)–Si(1)–Si(4) | 104.8(3) | Si(3)–Si(1)–Si(4) | 105.1(3) |
| Mn(1)–Si(5)–Si(6) | 111.0(3) | Mn(1)–Si(5)–Si(7) | 122.1(3) |
| Si(6)–Si(5)–Si(7) | 104.3(3) | Mn(1)–Si(5)–Si(8) | 110.6(3) |
| Si(6)–Si(5)–Si(8) | 104.8(3) | Si(7)–Si(5)–Si(8) | 102.5(3) |
| Mn(1)–O(1)–C(1) | 170.0(1) | Mn(1)–O(2)–C(101) | 165.0(1) |

bond distances, 2.642(6) and 2.662(6) Å, are comparable with those observed in **5**.

The Mn–O distances in **6**, 2.13(1) and 2.14(1) Å, are significantly longer than the Mn–O distances reported for $(CO)_5Mn(OCPhEt)$ (2.064(3) Å) and $(CO)_4(Ph_3As)Mn(OCPh_2)$ (average 2.04 Å) [15]. More relevant is a comparison to the Mn–O distances in the four-coordinate, Mn(II) aryloxide $Mn[O(2,4,6\text{-}^tBu_3\text{–}C_6H_2)]_2(NCMe)_2$, which are 1.910(6) Å [16]. The latter comparison is most consistent with the characterization of the Mn–O bonds in **6** as dative, rather than normal covalent bonds. The Mn–O–C angles are rather large, at 165(1) and 170(1)°. The inequivalent C=O distances of 1.24(2) and 1.29(2) Å are nearly the same as the analogous distance in free benzophenone (1.23 Å) [17], but are significantly shorter than the C–O distance observed for the ketyl complex $Ca(OCPh_2)_2(HMPA)_3$ (1.31(2) Å) [14]. The dihedral angles associated with both pairs of phenyl rings, 54.4 and 52.8°, are also similar to the corresponding parameter found in free benzophenone (56°) [17]. The measured C–C distances in the phenyl rings vary considerably between 1.30(4) and 1.48(4) Å, but in an apparently random manner. Thus, the metrical parameters for **6** are highly consistent with a Mn(II) center complexed by two benzophenone ligands which have not been significantly reduced by electron transfer.

### 3.5. Reactions of $[NEt_4]\{FeCl[Si(SiMe_3)_3]_2\}$ and $Mn[Si(SiMe_3)_3]_2(THF)_2$ (3) with π-acids

Coordinatively unsaturated silyl complexes of manganese and iron are in general reactive toward π-acids such as CO and CNXyl (Xyl = 2,6-$Me_2$–$C_6H_3$). A pure

product **7** was isolated from the reaction of $[NEt_4]\{FeCl[Si(SiMe_3)_3]_2\}$ [2] with carbon monoxide (Eq. (4)). Both $^1H$ and $^{13}C\{^1H\}$ NMR spectra reveal the presence of equivalent -$Si(SiMe_3)_3$ ligands, which is consistent with two possible geometries for a six-coordinate Fe center. One possible isomer has *cis*-$Si(SiMe_3)_3$ ligands and a *fac* arrangement of the CO ligands, while the other one has *trans* silyl groups with a *mer* grouping of the CO groups. The available spectroscopic data do not allow us to distinguish between these two possibilities, but we prefer the isomer with *trans* silyl groups based on steric considerations.

$$[NEt_4]\{FeCl[Si(SiMe_3)_3]_2\} \xrightarrow[OEt_2]{CO} [NEt_4]\{Fe(CO)_3[Si(SiMe_3)_3]_2Cl\} \quad (4)$$

**7**

Reactions of **3** with one or 2 equiv. of CNXyl produced light orange to red paramagnetic powders which analyzed (by hydrolytic degradation) as $Mn[Si(SiMe_3)_3]_2(CNXyl)(THF)$ (**8**). This reaction also produced an air-stable, yellow, diamagnetic complex that did not cleanly degrade by hydrolysis in benzene-$d_6$. However, this product was characterized as $(XylNC)_5Mn$-$Si(SiMe_3)_3$ (**9**) by NMR spectroscopy and mass spectrometry (Eq. (5)). As expected, the yield of this product increased with use of more CNXyl in the synthesis, but the yield of this reaction was not optimized. The formation of this product represents an interesting reduction of Mn(II) to Mn(I), but attempts to identify other redox products in the reaction, or other silicon-based products, were not successful. Complex **9** is similar to the stannyl derivative $(XylNC)_5MnSnPh_3$, reported by Cooper and coworkers [18].

$$Mn[Si(SiMe_3)_3]_2(THF)_2 \xrightarrow[pentane]{\text{excess CNXyl}} \begin{matrix} & CNXyl & \\ & | & \\ XylNC & Mn & Si(SiMe_3)_3 \\ & | & \\ XylNC & CNXyl & \end{matrix} \quad (5)$$

**9**

## 4. Conclusions

The neutral manganese and iron silyl complexes **3** and **4** are useful starting materials for the synthesis of various coordination compounds. Significantly, **3** is more reactive than the 1,2-dimethoxyethane derivative $Mn[Si(SiMe_3)_3]_2(DME)$ [2]. Ligands that behave primarily as σ-donors are observed to provide paramagnetic manganese silyl complexes of the type $Mn[Si(SiMe_3)_3]_2L_2$. The bis(benzophenone) complex **6** appears somewhat unusual as a compound of this type, in that it exhibits a dark blue color and a UV–Vis absorption spectrum that is similar to that for the benzophenone ketyl radical. However, the infrared and X-ray structural data clearly indicate that the benzophenone ligands in **6** are not significantly reduced. Presumably, the dark blue color of **6** results from a metal-to-ligand charge transfer transition. Reactions of coordinatively unsaturated, bis(silyl) complexes of Mn and Fe with the π-acids CNXyl and CO have been observed to give diamagnetic, coordinatively saturated complexes. For the reaction of CNXyl with **3**, a novel redox process occurs to produce a reduced iron center. Overall, the results reported here indicate that highly unsaturated compounds of the first row metals supported by the bulky silyl ligand -$Si(SiMe_3)_3$ exhibit a rich reaction chemistry. Future efforts will focus on exploitation of this chemistry in search of new chemical transformations.

## Acknowledgements

We acknowledge the National Science Foundation for their generous support of this work. We also thank Greg Mitchell for experimental assistance.

## References

[1] (a) T.D. Tilley, in: S. Patai, Z. Rappoport (Eds.), The Silicon-Heteroatom Bond (chapters 9 and 10), Wiley, New York, 1991, pp. 245–309;
(b) T.D. Tilley, in: S. Patai, Z. Rappoport (Eds.), The Chemistry of Organic Silicon Compounds (chapter 24), Wiley, New York, 1989, p. 1415;
(c) M.S. Eisen, in: S. Patai, Z. Rappoport (Eds.), The Chemistry of Organic Silicon Compounds (chapter 35), Wiley, New York, 1998, p. 2037;
(d) K.H. Pannell, H.K. Sharma, Chem. Rev. 95 (1995) 1351;
(e) J.Y. Corey, J. Braddock-Wilking, Chem. Rev. 99 (1999) 175;
(f) J.A. Reichl, D.H. Berry, Adv. Organomet. Chem. 43 (1999) 197.
[2] D.M. Roddick, T.D. Tilley, A.L. Rheingold, S.J. Geib, J. Am. Chem. Soc. 109 (1987) 945.
[3] G. Gutekunst, A.G. Brook, J. Organomet. Chem. 225 (1982) 1.
[4] D.F. Evans, T.A. James, J. Chem. Soc., Dalton Trans. (1979) 723.
[5] B.K. Nicholson, J. Simpson, W.T. Robinson, J. Organomet. Chem. 47 (1973) 403.
[6] G.S. Girolami, G. Wilkinson, A.M.R. Galas, M. Thorton-Pett, M.B. Hursthouse, J. Chem. Soc., Dalton Trans. (1985) 1339.
[7] D.E. Gindelberger, J. Arnold, Inorg. Chem. 32 (1993) 5813.
[8] P.B. Hitchcock, M.F. Lappert, W.-P. Leung, N.H. Buttrus, J. Organomet. Chem. 394 (1990) 57.
[9] (a) J.A. Gladysz, Acc. Chem. Res. 17 (1984) 326;
(b) D.L. Johnson, J.A. Gladysz, J. Am. Chem. Soc. 101 (1979) 6433;
(c) D.L. Johnson, J.A. Gladysz, Inorg. Chem. 20 (1981) 2508.
[10] J. Arnold, T.D. Tilley, J. Am. Chem. Soc. 109 (1987) 3318.
[11] R.J. McKinney, G. Firestein, H.D. Kaesz, Inorg. Chem. 14 (1975) 2057.
[12] E. Hayon, T. Ibata, N.N. Lichtin, M. Simic, J. Phys. Chem. 76 (1972) 2072.
[13] (a) K.J. Covert, P.T. Wolczanski, Inorg. Chem. 28 (1989) 4565;
(b) K.J. Covert, P.T. Wolczanski, S.A. Hill, P.J. Krusic, Inorg. Chem. 31 (1992) 66.

[14] Z. Hou, X. Jia, M. Hoshino, Y. Wakatsuki, Angew. Chem., Int. Ed. Engl. 36 (1997) 1292.
[15] H.-J. Haupt, G. Lohmann, U. Flörke, Z. Anorg. Allg. Chem. 526 (1985) 103.
[16] D. Meyer, J.A. Osborn, M. Wesolek, Polyhedron 9 (1990) 1311.
[17] E.B. Fleischer, N. Sung, S. Hawkinson, J. Phys. Chem. 72 (1968) 4311.
[18] T.L. Utz, P.A. Leach, S.J. Geib, N.J. Cooper, J. Chem. Soc., Chem. Commun. (1977) 847.